ORIGINAL ARTICLE

Quantitative and Dynamic ctDNA as a Biomarker of Response and Survival in Patients With Advanced Lung Squamous Cell Carcinoma Receiving Immunochemotherapy or Chemotherapy Alone

Fei Zhou, MD, PhD,[a,b] Jiao Zhang, MA,[c] Shengxiang Ren, MD, PhD,[b] Jianhua Chen, MD, PhD,[d] Feifei Li, MA,[c] Ting Ma, MA,[c] Yong Fang, MD, PhD,[e] Qiming Wang, MD, PhD,[f] Wenxiu Yao, MD, PhD,[g] Renhua Guo, MD, PhD,[h] Dongqing Lv, MD, PhD,[i] Shundong Cang, MD, PhD,[j] Xiaorong Dong, MD, PhD,[k] Huijuan Wang, MD, PhD,[l] Nong Yang, MD, PhD,[m] Yun Fan, MD, PhD,[n] Jiuwei Cui, MD, PhD,[o] Ziping Wang, MD, PhD,[p] Jianxing He, MD, PhD,[q] Yu S. Huang, PhD,[c] Weizhi Chen, PhD,[c] Li-Di Xu, PhD,[c] Caicun Zhou, MD, PhD[a,b,*]

[a]*Department of Medical Oncology, Shanghai East Hospital, Tongji University School of Medicine, Shanghai, People's Republic of China*
[b]*Department of Medical Oncology, Shanghai Pulmonary Hospital, Tongji University School of Medicine, Shanghai, People's Republic of China*
[c]*Genecast Biotechnology Co., Ltd. Wuxi, People's Republic of China*
[d]*Department of Medical Oncology-Chest, Hunan Cancer Hospital, Changsha, People's Republic of China*
[e]*Department of Medical Oncology, Sir Run Run Shaw Hospital Zhejiang University School of Medicine, Hangzhou, People's Republic of China*
[f]*Department of Oncology, Henan Cancer Hospital, Zhengzhou, People's Republic of China*
[g]*Department of Thoracic Oncology, Sichuan Provincial Cancer Hospital, Chengdu, People's Republic of China*
[h]*Department of Oncology, Jiangsu Province Hospital, Nanjing, People's Republic of China*
[i]*Department of Breath Internal Medicine, Taizhou Hospital of Zhejiang Province, Taizhou, People's Republic of China*
[j]*Department of Medical Oncology, Henan Provincial People's Hospital, Zhengzhou, People's Republic of China*
[k]*Cancer Center, Union Hospital of Tongji Medical College, Huazhong University of Science and Technology, Wuhan, Hubei, People's Republic of China*
[l]*Department of Respiration, Henan Cancer Hospital, Zhengzhou, Henan, People's Republic of China*
[m]*Department of Medical Oncology, Hunan Cancer Hospital, Changsha, Hunan, People's Republic of China*
[n]*Department of Medical Oncology, Zhejiang Cancer Hospital, Hangzhou, Zhejiang, People's Republic of China*
[o]*Cancer Center, the First Bethune Hospital of Jilin University, Changchun, Jilin, People's Republic of China*
[p]*Department of Medical Oncology, Beijing Cancer Hospital, Beijing, People's Republic of China*
[q]*Department of Thoracic Surgery and Oncology, the First Affiliated Hospital of Guangzhou Medical University, Guangzhou, Guangdong, People's Republic of China*

Received 4 December 2024; revised 31 March 2025; accepted 27 May 2025
Available online - XXX

ABSTRACT

Introduction: Although circulating tumor DNA (ctDNA) dynamics have been widely explored for therapeutic response assessment, standardized methodologies remain elusive. Here, we developed MinerVa-Delta, a novel approach to quantify ctDNA dynamics by calculating weighted mutation changes in samples with multiple tracked variants.

Methods: MinerVa-Delta was developed and analytically validated using serially diluted reference samples. The optimal cutoff was determined in a discovery cohort of 227 patients with advanced lung squamous cell carcinoma (LUSC) receiving programmed cell death protein 1 blockade

*Corresponding author.

Drs. F. Zhou and J. Zhang contributed equally to this work.

Address for correspondence: Caicun Zhou, MD, PhD, Department of Medical Oncology, Shanghai East Hospital, Tongji University School of Medicine, Shanghai, People's Republic of China, No. 1800, Yuntai Road, Pudong New Area, Shanghai, People's Republic of China. E-mail: caicunzhoudr@163.com

Cite this article as: Zhou F, Zhang J, Ren S, et al. Quantitative and dynamic ctDNA as a biomarker of response and survival in patients with advanced lung squamous cell carcinoma receiving immunochemotherapy or chemotherapy alone. *J Thorac Oncol* XXXX;X:XXXXXX

© *2025 International Association for the Study of Lung Cancer. Published by Elsevier Inc. All rights are reserved, including those for text and data mining, AI training, and similar technologies.*

ISSN: 1556-0864

https://doi.org/10.1016/j.jtho.2025.05.021

plus chemotherapy or chemotherapy alone and further validated in an independent cohort of 97 patients with LUSC treated with chemotherapy alone. Variants were de novo called in pretreatment samples using a 769-gene next-generation sequencing panel, serving as a basis for personalized variant tracking in posttreatment plasma after two cycles of treatment. We applied MinerVa-Delta to evaluate prognosis and therapeutic response in advanced LUSC.

Results: Patients classified as molecular responders (MinerVa-Delta $<30\%$) exhibited significantly improved outcomes compared with nonresponders (MinerVa-Delta $\geq 30\%$), with superior progression-free survival (hazard ratio $=$ 0.19, $p < 0.001$) and overall survival (hazard ratio $= 0.24$, $p < 0.001$). MinerVa-Delta displayed consistent prediction performance in the validation cohort. Furthermore, MinerVa-Delta accurately identified radiologic stable disease patients, a clinically heterogeneous population, who could benefit from initial treatment.

Conclusions: Our findings suggest MinerVa-Delta is feasible for evaluating treatment response in patients with advanced LUSC. Integrating ctDNA profiling with conventional imaging could enhance response assessment, particularly in radiologic stable disease patients, enabling more precise therapeutic decision-making.

© 2025 International Association for the Study of Lung Cancer. Published by Elsevier Inc. All rights are reserved, including those for text and data mining, AI training, and similar technologies.

Keywords: Lung squamous cancer; Treatment response; Circulating tumor DNA; PD-1 blockade; Chemotherapy

Introduction

Radiologic imaging technologies have long been used to assess therapeutic response and track posttreatment outcomes in patients with cancer. Despite being widely used in clinical practice and research, these imaging-based approaches have limitations, including inconsistency in image interpretation and technical constraints in visualizing malignancies at specific anatomical sites.[1,2] These challenges are exacerbated in immunotherapy, in which tumor enlargement or pseudoprogression may reflect treatment-induced immune activity rather than true disease progression,[3–5] rendering traditional size-based response criteria unreliable.[2,6] To address these challenges, circulating tumor DNA (ctDNA) has emerged as a promising alternative biomarker.

The utility of ctDNA for molecular response assessment has been extensively reviewed,[7,8] highlighting its advantages over traditional image-based approaches. Typically, ctDNA-based evaluation of molecular response involves quantifying ctDNA kinetics by comparing posttreatment or on-treatment time points with baseline. Serial monitoring of ctDNA in plasma, which tracks increases or decreases over time, has proven to be an effective disease-monitoring tool.[9,10] Coupled with next-generation sequencing (NGS) assays, various metrics have been developed, including the mean variant allele frequency (VAF),[11,12] maximum VAF,[10,13–16] and ctDNA concentration in terms of haploid genome equivalents per milliliter.[17,18]

Notably, a decrease or complete clearance of ctDNA within the first 3 to 9 weeks after treatment initiation has been found to be associated with favorable treatment outcomes.[7,13,19–21] ctDNA clearance or persistence classification is particularly useful for patients with early-stage cancer or when evaluating changes in a single targeted variant. For instance, our previous study found that patients with ctDNA clearance after adjuvant treatment experienced substantially improved survival compared with those with persistent ctDNA, highlighting the prognostic value of dynamic ctDNA assessment.[22] Yet, in patients with advanced cancer, complete clearance of ctDNA may not always occur. In such cases, a substantial reduction in ctDNA, despite minimal residual levels, can indicate a remarkable therapeutic response. Methods such as proportional change in ctDNA can account for both the relative change in ctDNA and the amount of residual ctDNA remaining at the on- or posttreatment time points. However, no consensus currently exists on the quantitative definition of "meaningful decrease" in ctDNA for classifying molecular responders.

Threshold values for ctDNA ratio changes used to select the treatment response group with good prognosis have varied widely, ranging from 25% to 90%. Furthermore, all the aforementioned VAF-based metrics have the limitation of not accounting for the uncertainty of VAF. Recently, a response classification called "ctDNA-RECIST" has been proposed,[23] on the basis of ctDNA measurements and confidence intervals (CIs), similar to the image-based Response Evaluation Criteria in Solid Tumors (RECIST) system.[24] However, the proposed five classification groups are complex and have not been prospectively validated.

In this proof-of-concept study, we proposed MinerVa-Delta as a novel approach to measure the ratio change of VAF while taking into account the depth and variance of VAF levels of each variant before and after treatment. The rationale for considering the depth and variance of VAF is that the reliability of VAF is related to the deduplicated depth and the allele frequency of the variant at both pretreatment and posttreatment time points.[25] The VAF SD (std) grows when allele frequency or depth is at low levels. Consequently, when computing the overall ctDNA ratio change for each sample, individual variant ratio change is assigned with a weight. The metric was

constructed and validated in two independent cohorts (CameL-Sq[21] and LIPUSU trials[26]) containing patients with advanced lung squamous cell carcinoma (LUSC) receiving first-line programmed cell death protein 1 (PD-1) blockade plus chemotherapy or chemotherapy alone. Herein, we present the design and analytical validation of the pretreatment plasma-informed MinerVa-Delta assay and illustrate the clinical utility of MinerVa-Delta-defined "molecular responder," aiming to identify patients with advanced LUSC who can benefit from first-line PD-1 blockade plus chemotherapy or chemotherapy alone.

Methods

Study Design and Patients

This study comprised two independent clinical trials. The CameL-Sq trial (NCT03668496) was a randomized, placebo-controlled, multicenter, double-blinded phase 3 trial. Enrolled patients were aged 18 to 75 years with stage IIIB to IV LUSC. Participants received first-line camrelizumab or matching placebo in combination with carboplatin plus paclitaxel for 4 to 6 cycles, followed by maintenance therapy with camrelizumab or placebo until disease progression.[21] The second trial, LIPUSU (NCT02996214), was a randomized phase 3 trial involving patients with advanced LUSC. Enrolled patients were randomly assigned to receive up to six cycles of paclitaxel liposome plus cisplatin or gemcitabine plus cisplatin as first-line treatment.[26] We refer to these two cohorts as cohort A and cohort B hereafter.

Plasma samples were collected at two time points: pretreatment baseline (C0) and posttreatment (C1) after 6 weeks or two cycles of treatments. The rationale for selecting the post–two-cycle time point was our previous observation that the mean VAF at this stage significantly distinguished patients with a partial response (PR) from those with stable disease ($p = 0.003$) or progressive disease (PD) ($p = 0.004$).[21] In addition, for cohort A, baseline tumor biopsies were collected and somatic mutations were analyzed. Patients with matched tumor tissue (C0) and plasma samples at both C0 and C1 were included. The two cohorts comprised 227 and 97 patients, respectively. Time-matched peripheral blood leukocytes at C0 were prospectively collected to filter out clonal hematopoiesis (CH).

For MinerVa-Delta model development on the basis of ctDNA dynamic changes, we used samples from cohort A, which included paired pretreatment tumor biopsies and plasma samples. The plasma-informed MinerVa-Delta model established in this cohort was independently validated in cohort B.

This study was conducted in accordance with the principles of the Declaration of Helsinki and the Good Clinical Practice guidelines of the International Council for Harmonization. The study protocols and all amendments were reviewed by independent ethics committees or institutional review boards at each center, and all patients provided written informed consent.

End Points Assessment

Tumor response assessment followed the RECIST version 1.1 criteria.[24] Assessments were carried out after 2 treatment cycles (6 wk) and repeated every two treatment cycles. The objective response rate, including PR, stable disease, and PD, was assessed.[24] Progression-free survival (PFS) was defined as the time from randomization to the first RECIST-defined disease progression or death, whichever occurred first. Overall survival (OS) was defined as the time from randomization to death from any cause. Patients without death or progression during the study period were considered censored.

ctDNA Analysis, De Novo Calling and Minerva Tracking

DNA isolation from plasma samples or biopsies, library preparation, and NGS were conducted at Genecast Biotechnology Co. Ltd. Detailed experimental procedures have been described in the Supplementary Methods. Comprehensive genomic profiling, including single nucleotide variant and indels, was analyzed using MinerVa, a 769-gene NGS panel (Genecast, Wuxi, People's Republic of China).[19,21] If tumor biopsies were available, variants detected in biopsies were used for tracking in pretreatment plasma; otherwise, a de novo calling approach was used in pretreatment plasma. Variants identified in pretreatment plasma served as the basis for personalized tracking in posttreatment plasma (Fig. 1).

The de novo calling method was adapted from our previously published approach,[21] with minor adjustments for cohort B, in which unique molecular identifiers (UMIs) were used. To minimize background noise and ensure high-quality variants for tracking, several filtering steps were applied. First, non-hotspot mutations were excluded if they exhibited a VAF less than 0.1% or a p value greater than 0.001. Second, variants with duplex count of less than 3 (in UMI-based samples) or VAF of less than 1% (in non-UMI samples) were excluded to eliminate low-confidence calls. Finally, paired buffy coat (BC) and plasma ctDNA analysis were conducted to remove germline and CH-associated variants. Specifically, plasma variants with VAF less than 1%, which were also present in BC were filtered out if the p value from the Fisher's exact test was greater than 0.01, whereas variants with VAF of 1% or more were excluded if the ratio of VAF in baseline plasma to VAF in BC was 5 or less.

Genotyping for tracking posttreatment variants was performed as described,[18] with a significant threshold of p less than 0.01 to determine a positive variant.

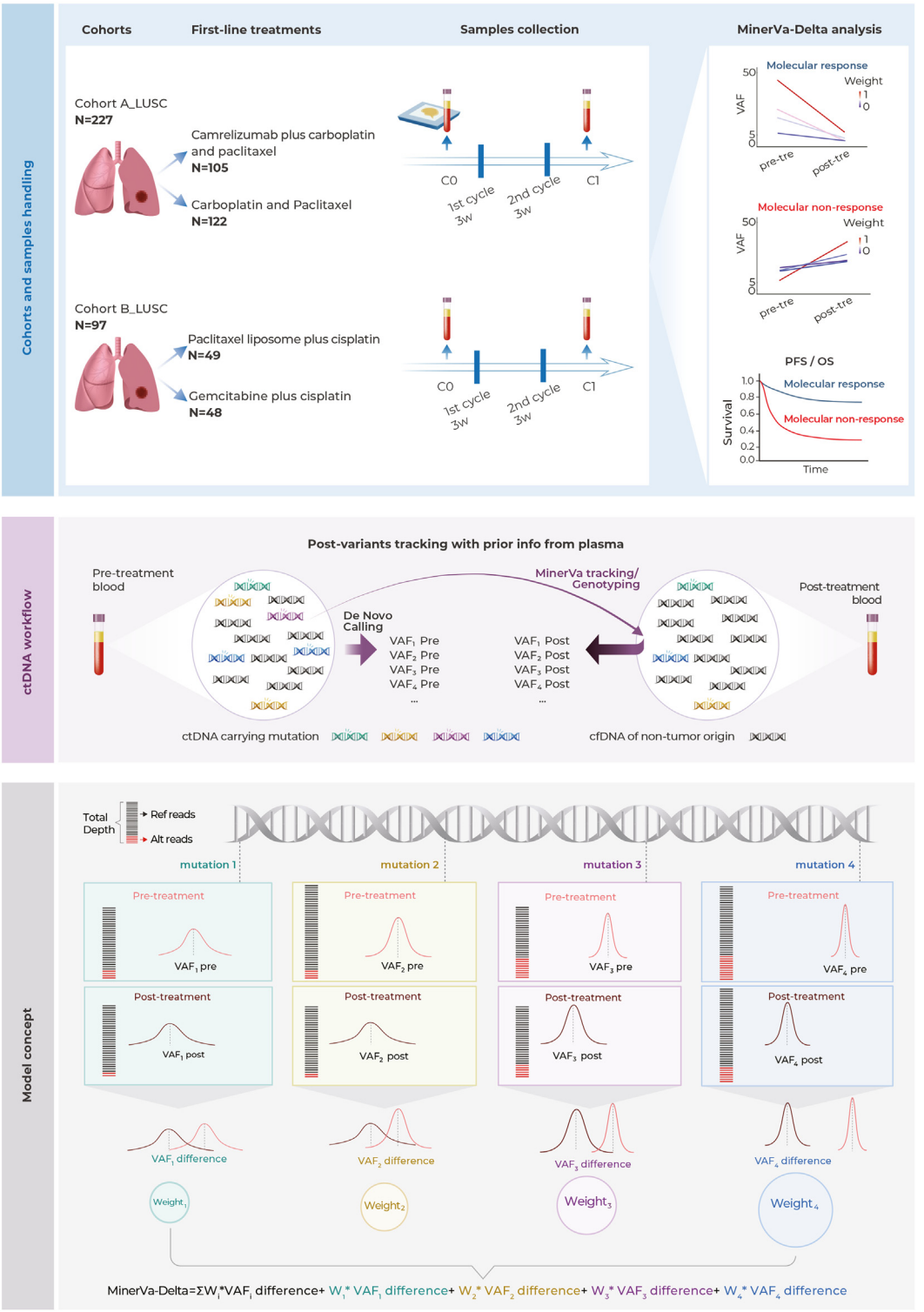

Figure 1. Study design, ctDNA workflow and conceptual framework for establishing MinerVa-Delta. This study included two cohorts: cohort a (discovery cohort) and cohort B (validation cohort). Plasma samples were collected at two time points: C0 (before initial treatment) and C1 (after two cycles of treatments for cohort A and B). MinerVa-Delta for each patient was defined as the sum of normalized weighted differences in VAFs for each trackable variant. The VAF difference was calculated as ratio change of posttreatment to pretreatment VAF (VAF_{post}/VAF_{pre}). The weight assigned to each variant's ratio change was positively associated with sequencing depth, VAF levels, and deltaVAF (VAF post-VAF pre) (see Methods section). This figure illustrates the clinical application of MinerVa-Delta in evaluating treatment response and predicting OS and PFS in patients with advanced lung squamous cell carcinoma receiving first-line treatments. ctDNA, circulating tumor DNA; VAF, variant allele frequencies; OS, overall survival; PFS, progression-free survival. Figures were partially created with BioRender.com.

The analytical performance was assessed for both de novo calling and genotyping approaches (detailed in the Supplementary Methods).

Establishment of MinerVa-Delta model

We developed a ctDNA dynamic change metric by utilizing pretreatment and posttreatment ctDNA. First, we computed the VAF ratio change for each mutation using the formula: VAF_{post}/VAF_{pre}. Second, instead of calculating the mean VAF change, we assigned differential weights to mutations in samples with multiple tracked variants. To account for VAF uncertainty, we assigned a specific weight to each locus that is inversely proportional to the std of VAF. In addition, we incorporated the sequencing coverage's impact on VAF uncertainty by making the uncertainty measure inversely proportional to the sequencing coverage. We estimated the std for each VAF through simulation and verified it using the reference samples.

In our approach, we assumed that the number of reads supporting the mutant allele (alternative allele counts) at each specific locus follows a binomial distribution $X \sim B(D, p)$. Here, D represents the deduplicated depth and p represents the probability of obtaining the expected X.

The variance of X is expected to be:

$$var(X) = Dp(1-p) = EX^2 - (EX)^2 = EX^2 - D^2p^2 \quad (1)$$

From (1), we obtained

$$EX^2 = Dp(1-p) + D^2p^2 \quad (2)$$

Because D is a constant, therefore,

$$E(X/D) = EX/D = p \quad (3)$$

Then, from both (2) and (3), the variance of X/D is derived as follows:

$$var(X/D) = E\left(X^2/D^2\right) - (E(X/D))^2 = EX^2 \Big/ D^2 - p^2$$

$$= \left(Dp(1-p) + D^2p^2\right) / D^2 - p^2 = p(1-p)/D \quad (4)$$

Therefore, we finally obtained \cr

$$std(X/D) = std(VAF) = \sqrt{p(1-p)}/\sqrt{depth} \quad (5)$$

Reference samples were used to verify the expected std(VAF).

After that, the std(VAF) derived from (5) was used for calculating the weight of each locus change with the following formula:

$$\tilde{w} = \left|VAF_{pre} - VAF_{post}\right| \Big/ \sqrt{std\left(VAF_{pre}\right) + std\left(VAF_{post}\right)} \quad (6)$$

For samples with multiple tracked mutations, the weight for the i th mutation was further normalized as:

$$w_i = \tilde{w}_i / \Sigma_{i=1}^{n} \tilde{w}_i \quad (7)$$

In the final step, for each sample, MinerVa-Delta was estimated by the formula MinerVa-Delta:

$$\text{MinerVa} - \text{Delta} = \sum_{i=1}^{n} \left(w_i * VAF_{post}^{i} \Big/ VAF_{\text{pre}}^{i} \right) \quad (8)$$

The concordance of the estimated weighted ratio change derived from MinerVa-Delta with the observed ratio change was assessed (detailed in Supplemental Methods).

Statistical Analyses

Survival curves were estimated using the Kaplan-Meier method. Hazard ratios (HRs) for OS and PFS were calculated using univariate or multivariate Cox proportional hazard models while p-values were calculated using the log-rank test. The Kruskal-Wallis test was applied to assess differences among more than two groups. For pairwise comparisons following a significant Kruskal-Wallis test, the Dunn test was used, with p-values adjusted using the Benjamini-Hochberg method to control for multiple testing. All hypothesis testing was two-sided, with a significance threshold of $p < 0.05$. All analyses were performed in R, version 4.1.3 (R Core Team, Vienna, Austria). Prognosis analysis was conducted using the survival and survminer R packages. Receiver operating characteristic analysis was performed using the timeROC R package.[27]

Results

Design and Technical Verification of MinerVa-Delta

We developed a plasma-informed MinerVa-Delta model (Fig. 1) to address two clinical needs: (1) improving prognosis evaluation for patients with advanced LUSC after treatment, especially after immunochemotherapy, through a refined molecular response model; and (2) measuring treatment response in patients without available tissue. The specific MinerVa-Delta algorithm is described in the Methods section.

The analytical performance of the de novo calling and genotyping method was assessed separately. During an analytical evaluation with a series of diluted standard samples containing 12 mutations with known VAF, the 95% limit of detection for the UMI-based de novo calling approach was 0.42% (95% confidence interval [CI]: 0.41%–0.45%), whereas, for the non–UMI-based method, it was 1.43% (95% CI: 1.39%–1.47%) (Supplementary Table 1). The 95% limit of detection

for genotyping was determined to be 0.19% (95% CI: 0.17%–0.21%) (Supplementary Table 2). Cross-patient validation further revealed that the specificity of genotyping reached 99.86% (95% CI: 99.84%–99.88%) (Supplementary Table 3).

To simultaneously evaluate the accuracy of both de novo calling and genotyping, another series of diluted standard samples containing 687 known single nucleotide variants and indels were analyzed. The VAF of these expected mutations ranged from 0.029% to 100%, with the average VAF calculated from three replicates of each variant. As VAF decreased, the deviation of VAF increased. Genotyping identified 82% (n = 563) of expected variants, and de novo calling identified 59% (n = 408). For mutations with VAF greater than 0.1% (n = 475), de novo calling identified 85%, and genotyping detected 99%. The observed VAF revealed high concordance with the expected VAF (Pearson correlation coefficient: 0.94, $p < 0.001$) (Supplementary Fig. 1*A*).

The core element of MinerVa-Delta was assigning weight to the ratio change of each tracking variant. We then proceeded to evaluate the estimation accuracy of MinerVa-Delta by comparing the algorithm-computed ratio reduction (observed ratio change) with the expected ratio reduction, which was calculated on the basis of the actual dilution ratio (concentration of postdiluted sample/concentration of prediluted sample). Notably, the observed ratio reduction estimated by the MinerVa-Delta algorithm revealed a significant correlation with the expected ratio reduction, with a Spearman's correlation of 0.97 ($p < 2.2e^{-16}$) (Supplementary Fig. 1*B*).

Patient Characteristics and Pretreatment ctDNA Detection

This study used data from two independent prospective clinical trials involving individuals with advanced LUSC (Fig. 1). Patient characteristics are summarized in Supplementary Table 4. The two cohorts were comparable in terms of age, stage, and sex distribution. The average baseline ctDNA detection rate was 85%.

MinerVa-Delta Effectively Divided Patients Into Molecular Response and Nonresponse Groups

In cohort A, ctDNA positivity was 88% (199 of 227 patients) (Fig. 2*A*), with similar detection rates across clinical arms. MinerVa-Delta was used to calculate the weighted ctDNA ratio change before and after treatment for all tracked mutations per patient, as described in the Methods. Briefly, de novo calling identified pretreatment plasma variants, which were then used as a basis for personalized posttreatment plasma variant detection.

In cohort A, patients with CR or PR (n = 84) had significantly lower MinerVa-Delta levels than those with stable disease (n = 89) ($p < 0.0001$) or PD (n = 24) ($p < 0.0001$). In addition, stable disease patients had significantly lower MinerVa-Delta levels than PD patients ($p = 0.012$) (Fig. 2*B*). We then determined the MinerVa-Delta threshold for distinguishing molecular response from nonresponse groups using cohort A as a discovery set. Among cutoffs ranging from 5% to 95%, a 30% threshold best predicted OS, yielding the lowest HR of 0.24 (95% CI: 0.16–0.35, $p < 0.001$) (Fig. 2*C*). Meanwhile, MinerVa-Delta's prediction for PFS saturated after 30% (Fig. 2*D*), establishing 30% as the threshold for distinguishing molecular responders (MinerVa-Delta less than 30%) from nonresponders (MinerVa-Delta ≥30%). Using normalized weights of ratio changes for each variant, we graphically depicted representative molecular responders (Supplementary Fig. 2*A*) and nonresponders (Supplementary Fig. 2*B*). The sum of differentially weighted ratio changes determined the treatment response for each patient (Fig. 1). Consequently, 41 of 199 patients (21%) were classified as molecular nonresponders, whereas 158 (79%) were molecular responders. Molecular responders had significantly lower disease progression risk (HR = 0.19, 95% CI: 0.13–0.28, $p < 0.001$) and death risk (HR = 0.24, 95% CI: 0.16–0.35, $p < 0.001$) (Fig. 2*E* and *F*). Multivariate analysis confirmed MinerVa-Delta as a strong predictor for PFS (HR = 0.23, 95% CI: 0.15–0.34, $p < 0.001$) (Fig. 2*G*) and OS (HR = 0.25, 95% CI: 0.16–0.38, $p < 0.001$) (Fig. 2*I*), accounting for 53.92% (PFS) (Fig. 2*H*) and 60.49% (OS) (Fig. 2*J*) of predictive power. Notably, treatment regimen (PD-1 blockade plus chemotherapy versus chemotherapy alone) and programmed death-ligand 1 expression (tumor proportion score ≥1% versus <1%), identified as key predictors in univariate analysis (Supplementary Fig. 2*C*), remained significant PFS predictors in multivariate analysis (Supplementary Fig. 2G). In addition, programmed death-ligand 1 expression and liver metastasis were independently associated with OS in multivariate analysis (Fig. 2*I*, Supplementary Fig. 2*D*), accounting for 25.16% of OS predictive power (Fig. 2*J*).

We further questioned whether incorporating previous information from tumor tissue for variant tracking, termed the tumor-informed strategy, would yield comparable performance to the plasma-informed approach. As expected, the tumor-informed strategy achieved a higher detection rate of 99.6% (226 of 227 patients) (Supplementary Fig. 3*A*). The molecular response rate was slightly higher in the PD-1 blockade plus chemotherapy arm (87%, 91 of 105 patients) compared with the chemotherapy-only arm (74%, 90 of 121 patients), consistent with observations from the plasma-informed strategy (Fig. 2*A*). Notably, the tumor-informed MinerVa-Delta metric exhibited comparable classification performance in predicting both PFS and OS to the plasma-informed MinerVa-Delta metric across the entire

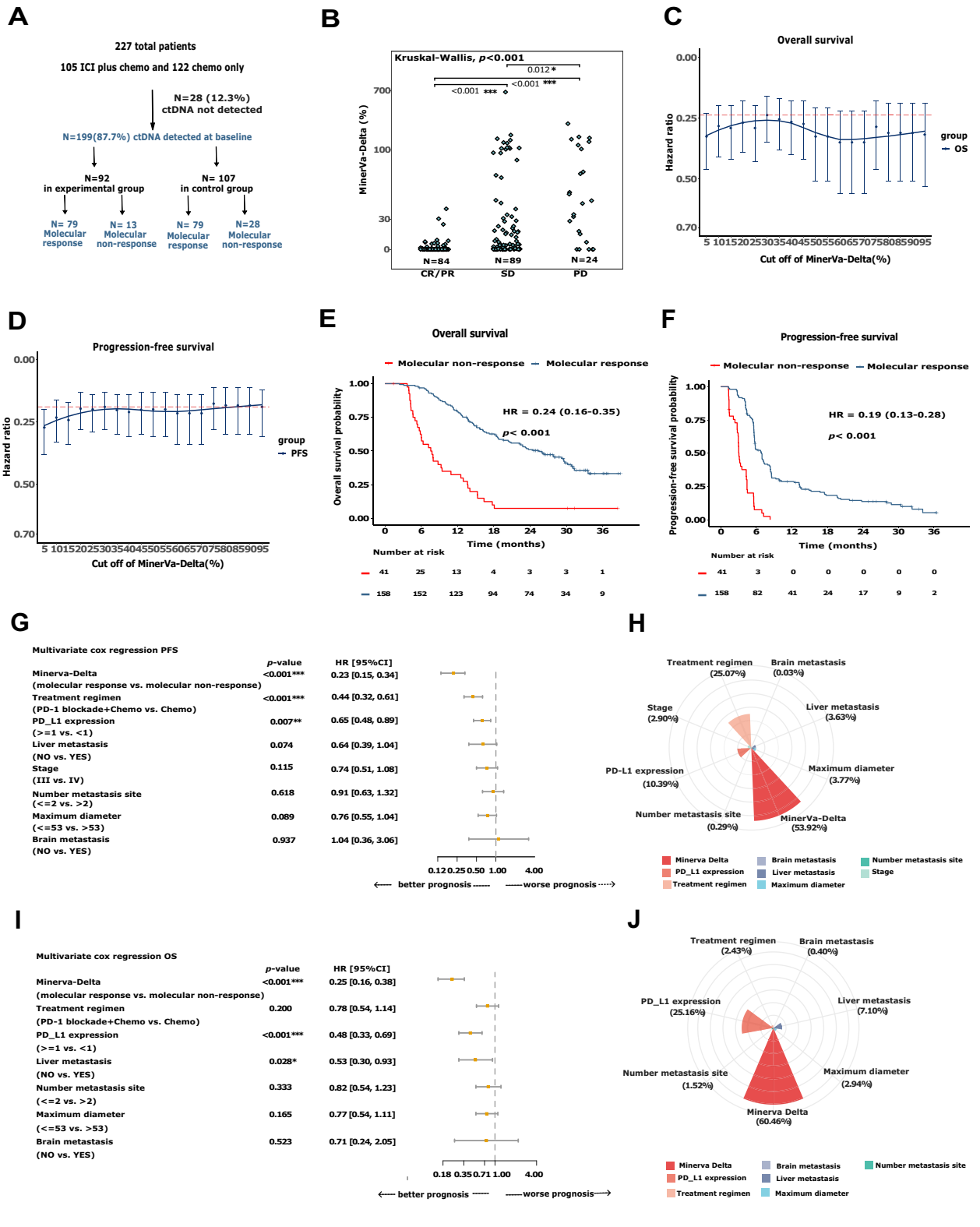

Figure 2. MinerVa-Delta metric cutoff determination and clinical performance. Variants de novo called in pretreatment plasma were used for variant detection in posttreatment plasma. (*A*) Pretreatment ctDNA detection rates in all patients and each treatment arm in cohort A, along with the number of patients classified as molecular responders and nonresponders using MinerVa-Delta. (*B*) Association of MinerVa-Delta with ORR (CR or PR versus stable disease versus PD). (*C–D*) HR comparison across MinerVa-Delta cutoffs ranging from 5% to 95% for both end points OS and PFS were evaluated. (*E–F*) Kaplan-Meier curves illustrating the prognosis of the molecular response group (MinerVa-Delta <30%, dark blue line) in

ARTICLE IN PRESS

cohort A (Supplementary Fig. 3*B*). Furthermore, among the 199 patients with results from both strategies, the tumor-informed and plasma-informed approaches exhibited similar time-dependent areas under the curve up to 3 years (Supplementary Fig. 3*C*). We then compared the prediction performance of MinerVa-Delta to mean VAF-based metrics at 30% and 50% ratio change cutoffs, which have been used in previous studies.[11,12] As expected, MinerVa-Delta outperformed these mean VAF-based metrics at both 30% and 50% cutoffs, displaying superior C-index values and better predictive performance for both PFS and OS (Supplementary Table 5).

Validation of MinerVa-Delta in an Independent Cohort

The prediction performance of MinerVa-Delta was further validated in another independent cohort B including patients with advanced LUSC receiving first-line chemotherapy. Baseline ctDNA positivity was 78% for the entire cohort (76 of 97 patients), with 38 patients in each of the paclitaxel liposome plus cisplatin and gemcitabine plus cisplatin arms (Fig. 3*A*). In cohort B, MinerVa-Delta levels were also associated with tumor response (CR or PR versus stable disease versus PD, $p < 0.0001$) (Fig. 3*B*). Using the same 30% cutoff, 54 patients (71%) were classified as molecular responders and 22 patients (29%) as molecular nonresponders. Molecular response status significantly predicted PFS (HR = 0.05, 95% CI: 0.02–0.13, $p < 0.001$) and OS (HR = 0.12, 95% CI: 0.06–0.24, $p < 0.001$) (Fig. 3*C* and *D*). These results indicate that patients in the molecular nonresponse group have approximately 20 times higher risk of disease progression and 8.3 times higher mortality risk. Multivariate analysis confirmed that MinerVa-Delta independently predicted PFS (HR = 0.06, 95% CI: 0.03–0.14, $p < 0.001$) and OS (HR = 0.12, 95% CI: 0.06–0.24, $p < 0.001$) in cohort B (Supplementary Fig. 4).

MinerVa-Delta Accurately Differentiated RECIST-Defined Stable Disease Patients

Although current clinical guidelines recommend maintaining the original treatment for patients classified as having stable disease on the basis of RECIST criteria, how to individually manage these patients remains a critical medical concern, particularly for those receiving PD-1 blockade treatment. We, therefore, evaluated the clinical performance of MinerVa-Delta in radiologic stable disease patients. The results revealed that MinerVa-Delta could further reclassify stable disease patients. In cohort A, 66 of 89 (74%) stable disease patients were classified as molecular responders, whereas in cohort B, 8 of 13 (61%) stable disease patients were molecular responders. In this stable disease subgroup analysis, molecular responders and nonresponders exhibited significantly different prognoses in both cohorts (cohort A: HR = 0.28, $p < 0.001$; cohort B: HR = 0.16, $p = 0.007$), whereas molecular nonresponders behaved similar outcomes to PD patients ($p = 0.721$ and not applicable for cohort A and cohort B, respectively) (Fig. 4*A* and *B*).

A slightly better differentiation was observed in the PD-1 blockade plus chemotherapy arm (HR = 0.18, $p < 0.001$) compared with the chemotherapy arm (HR = 0.40, $p = 0.003$) (Fig. 4*C* and *D*). Furthermore, molecular responders within the stable disease group had significantly better OS compared with molecular nonresponders within the stable disease group (Supplementary Fig. 5*A*–*D*). In summary, patients with radiologic stable disease but MinerVa-Delta–defined molecular response may benefit from continuing initial treatment. Conversely, patients with radiologic stable disease and molecular nonresponse have similar PFS and OS to patients with PD according to RECIST (Fig. 4*A*–*D*, Supplementary Fig. 5*A*–*D*), implying that this subgroup may need to consider changing treatment options (Fig. 4*E*).

MinerVa-Delta Better Stratified Patients Treated With PD-1 Blockade Plus Chemotherapy

We observed superior performance of MinerVa-Delta in the PD-1 blockade plus chemotherapy arm compared with the chemotherapy-only arm. In the PD-1 blockade plus chemotherapy arm, molecular responders exhibited significantly improved PFS and OS (HR = 0.13, 95% CI: 0.07–0.26, $p < 0.001$ for PFS; HR = 0.11, 95% CI: 0.05–0.23, $p < 0.001$ for OS), which were numerically better than those in the chemotherapy-only arm (HR = 0.27, 95% CI: 0.17–0.44, $p < 0.001$ for PFS; HR = 0.35, 95% CI: 0.21–0.57, $p < 0.001$ for OS) (Fig. 5*A* and *B*). The interactive p values were 0.033 for PFS and 0.008 for OS, indicating that MinerVa-Delta effectively identified patients who could receive durable clinical benefit from the addition of PD-1 blockade treatment. Similarly, molecular responders exhibited improved PFS and OS in both arms using tumor-informed strategies, though the treatment interaction was significant only for PFS (interactive p value = 0.028 for PFS and 0.093 for OS) (Fig. 5*C* and *D*).

Given that RECIST remains the golden standard for tumor response assessment, we further compared the performance of MinerVa-Delta versus RECIST in predicting

comparison with molecular nonresponse group (MinerVa-Delta $\geq$ 30%, red line) for OS and PFS. (*G*) Multivariate forest plot illustrating MinerVa-Delta and clinical parameters for PFS prediction. (*H*) Relative contribution of all clinical parameters and MinerVa-Delta to PFS prediction in multivariate Cox analysis. (*I*) Multivariate forest plot illustrating MinerVa-Delta and clinical parameters for OS prediction. (*J*) Relative contribution of all clinical parameters and MinerVa-Delta to OS prediction in multivariate Cox analysis. ORR, objective response rate; CR, complete response; PR, partial response; SD, stable disease; PD, progressive disease; HR, hazard ratio.

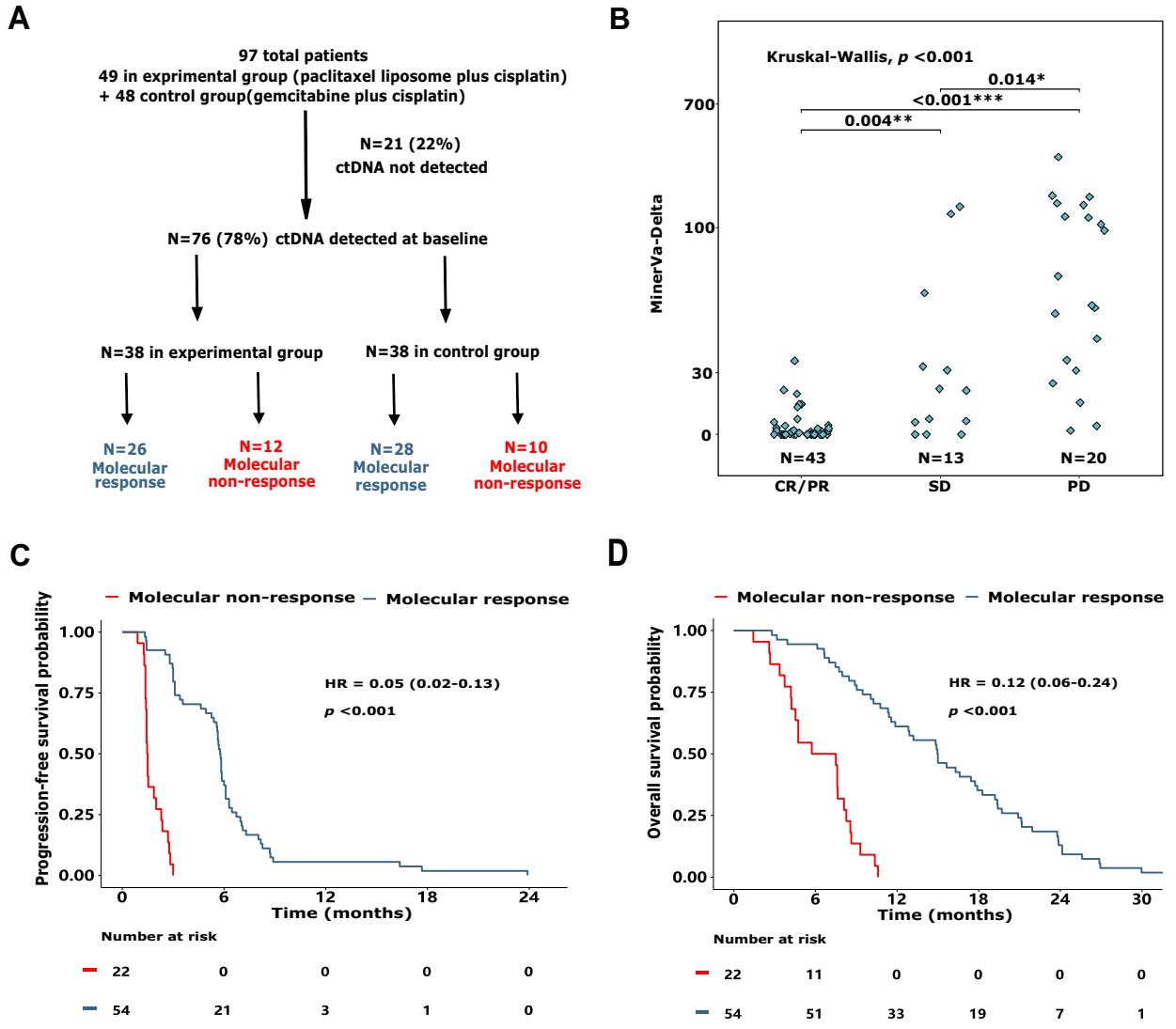

Figure 3. MinerVa-Delta metric performance in independent cohort B. (*A*) Pretreatment ctDNA detection rates in all patients and each treatment arm in cohort B, along with the number of patients classified as molecular response and nonresponse using MinerVa-Delta. (*B*) Association of MinerVa-Delta with ORR (CR or PR versus stable disease versus PD). (*C-D*) Kaplan-Meier curves illustrating the prognosis of the molecular response group (dark blue line) in comparison with molecular nonresponse group (red line) for PFS (*C*) and OS (*D*). CR, complete response; PR, partial response; SD, stable disease; PD, progressive disease; HR, hazard ratio; ctDNA, circulating tumor DNA; OS, overall survival; PFS, progression-free survival; ORR, objective response rate.

PFS and OS. Notably, MinerVa-Delta achieved numerically better performance in predicting both PFS (HR = 0.19 versus 0.31) and OS (HR = 0.24 versus 0.46) across the entire patient population in cohort A (Fig. 5*E* and *F*). Incorporating MinerVa-Delta with RECIST significantly improved prediction accuracy for PFS and OS compared with RECIST alone (Supplementary Fig. 6*A* and *B*).

When comparing the prediction effectiveness of MinerVa-Delta and RECIST in the PD-1 blockade plus chemotherapy arm and chemotherapy arm separately, we found that MinerVa-Delta performed better than RECIST in the PD-1 blockade plus chemotherapy arm (HR = 0.14 versus HR = 0.46 for PFS and HR = 0.12 versus HR = 0.41 for OS) (Fig. 5*E* and *F*). Meanwhile, in the chemotherapy-only arm, MinerVa-Delta exhibited similar prediction effectiveness to RECIST for PFS (HR = 0.27 for both) and relatively better performance for OS (HR = 0.35 versus 0.53) (Fig. 5*E* and *F*). Furthermore, similar prediction effectiveness of MinerVa-Delta and RECIST was observed in cohort B, including patients receiving chemotherapy alone (Supplementary Fig. 6*C*).

Discussion

In this study, we developed and validated a proof-of-concept tool named MinerVa-Delta, which quantifies

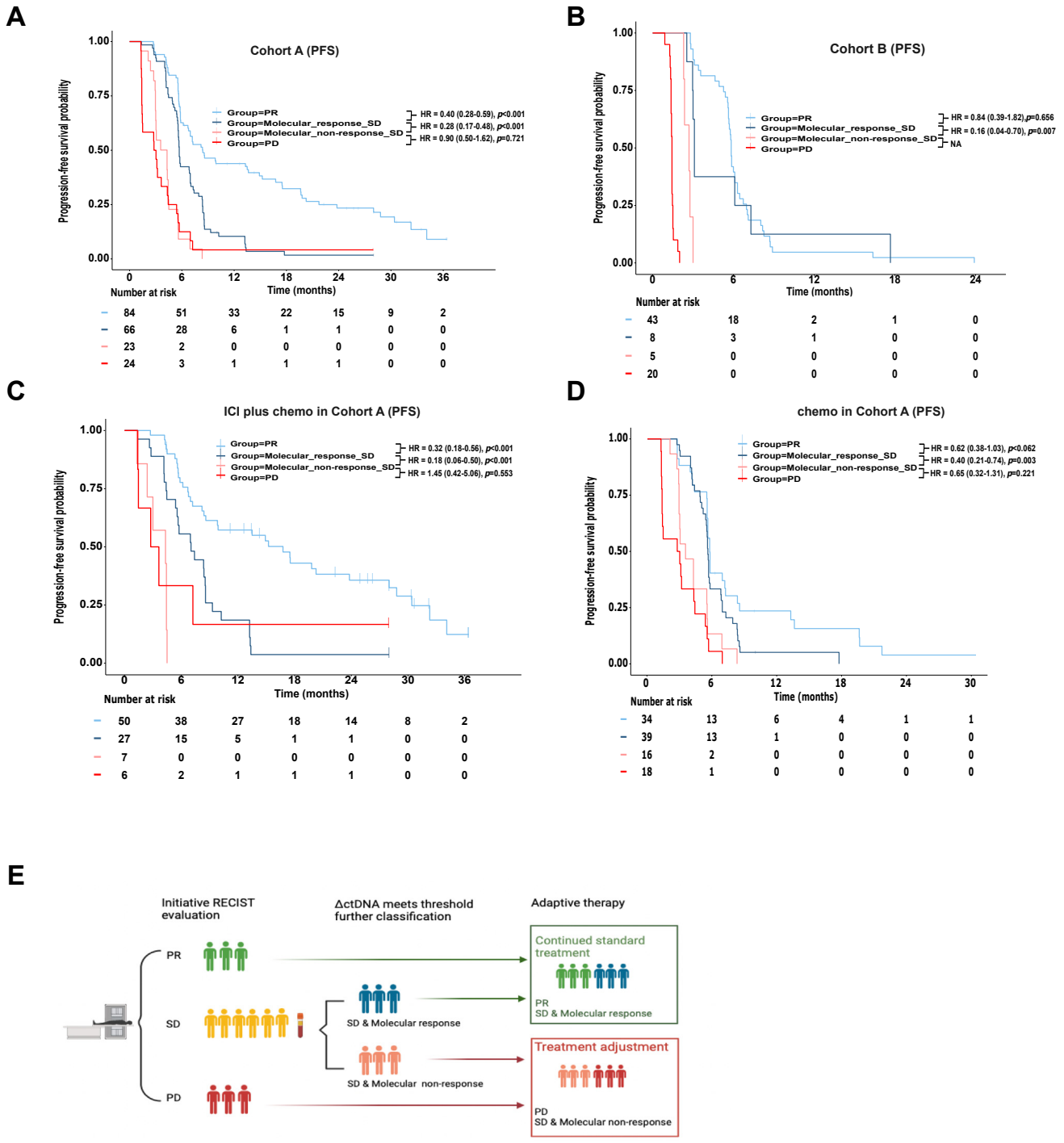

Figure 4. MinerVa-Delta differentiated RECIST-defined stable disease patients. Kaplan-Meier curves comparing the prognosis of PR patients (light blue line), molecular response plus stable disease group (dark blue line), molecular nonresponse group (pink line), and PD patients (red line) for predicting PFS in cohort A (*A*), cohort B (*B*), PD-1 blockade plus chemotherapy arm in cohort A (*C*) and chemotherapy-only arm in cohort A (*D*). The molecular response and molecular nonresponse groups were defined by MinerVa-Delta. HR, 95% CI, and *p* values were calculated to compare the molecular response plus stable disease group with molecular nonresponse plus stable disease group. (*E*) Proposed flowchart of incorporating ctDNA kinetics into standard treatment management. Stable disease patients defined through RECIST evaluation could be further classified using threshold ΔctDNA levels into molecular response and molecular nonresponse groups. Stable disease patients with a molecular response, together with those initially evaluated as PR, may continue with standard therapy. Meanwhile, stable disease patients with a molecular nonresponse, together with those initially evaluated as PD, may consider treatment adjustment. RECIST, Response Evaluation Criteria in Solid Tumors; PR, partial response; SD, stable disease; PD, progressive disease; CI, confidence interval; HR, hazard ratio; PFS, progression-free survival; PD-1, programmed death-ligand 1; ctDNA, circulating tumor DNA.

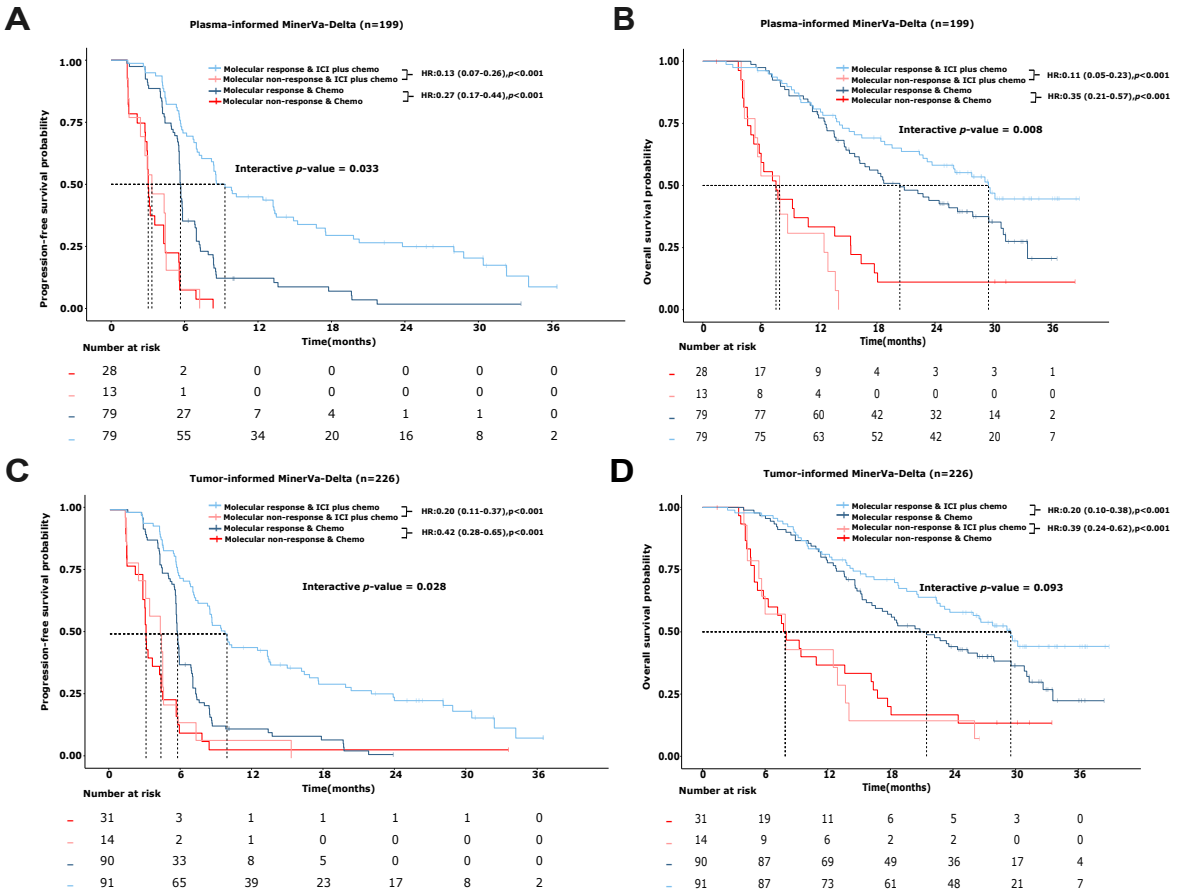

E

Univariate cox regression PFS

Group	Stratification	No. of responders (%)	*p*-value	HR [95%CI]
All patients	Molecular response	157 (79.7%)	<0.001***	0.19 [0.13, 0.29]
All patients	RECIST response	173 (87.8%)	<0.001***	0.31 [0.20, 0.48]
ICI + Chemo	Molecular response	78 (86.7%)	<0.001***	0.14 [0.07, 0.28]
ICI + Chemo	RECIST response	84 (93.3%)	0.092	0.46 [0.19, 1.16]
Chemo only	Molecular response	79 (73.8%)	<0.001***	0.27 [0.17, 0.44]
Chemo only	RECIST response	89 (83.2%)	<0.001***	0.27 [0.16, 0.46]

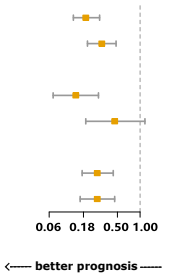

F

Univariate cox regression OS

Group	Stratification	No. of responders (%)	*p*-value	HR [95%CI]
All patients	Molecular response	157 (79.7%)	<0.001***	0.24 [0.16, 0.36]
All patients	RECIST response	173 (87.8%)	0.001**	0.46 [0.28, 0.74]
ICI + Chemo	Molecular response	78 (86.7%)	<0.001***	0.12 [0.06, 0.25]
ICI + Chemo	RECIST response	84 (93.3%)	0.049*	0.41 [0.16, 1.03]
Chemo only	Molecular response	79 (73.8%)	<0.001***	0.35 [0.21, 0.57]
Chemo only	RECIST response	89 (83.2%)	0.025*	0.53 [0.30, 0.93]

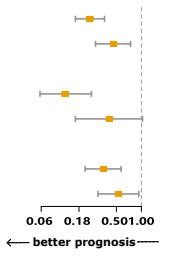

Figure 5. MinerVa-Delta better stratified patients treated with PD-1 blockade plus chemotherapy. (*A*-*D*) Kaplan–Meier curves illustrating prognostic differences between molecular responders (blue) and molecular nonresponders (red) in both PD-1 blockade plus chemotherapy arm (light blue, light red) and the chemotherapy-only arm (dark blue, dark red). The analyses were performed using plasma-informed (*A*: PFS, *B*: OS) and tumor-informed strategies (*C*: PFS, *D*: OS). HRs, 95% CI, and interaction *p* values were calculated using Cox proportional hazards model, with *p* values assessed by log-rank test. (*E* and *F*)

ctDNA dynamic changes, providing valuable insights for monitoring cancer treatment responses. MinerVa-Delta effectively classified patients with LUSC receiving first-line PD-1 blockade plus chemotherapy or chemotherapy alone into molecular responders and nonresponders, revealing significant differences in PFS and OS between the two groups. More importantly, MinerVa-Delta accurately identified radiologic stable disease patients, a clinically heterogeneous population, who could benefit from initial treatment. This makes it a valuable supplement to the current image-based RECIST classification system. A key advantage of this model is its ability to provide accurate results even in the absence of tumor tissue.

Accurately identifying patients with cancer likely to benefit from therapies in a timely manner is a crucial clinical question. Early prediction of treatment response would enable personalized therapy, ensuring patients receive the most effective treatment while minimizing adverse effects. It would also facilitate timely treatment adjustment for nonresponders. The prognostic value of pretreatment ctDNA VAF has been controversial, with some studies supporting its association with outcomes[11,17,28] whereas others find no significant correlation, particularly in LUSC.[19,29] In the LIPUSU trial (cohort B), although we found that pretreatment ctDNA was associated with survival outcomes,[30] ctDNA kinetic changes between pre- and on- treatment exhibited better separation of patients, identifying those with worse prognosis. This suggests that incorporating on-treatment data yields a better evaluation of treatment responses. Furthermore, for patients with advanced cancer, ctDNA clearance is rare. In such cases, defining molecular response on the basis of dynamic ctDNA changes between baseline and early on-treatment samples seems more appropriate than relying solely on ctDNA clearance.

Although our findings align with other proof-of-concept studies, most of these studies focused on assessing maximum VAF,[10,13–16,31,32] which is susceptible to stochastic sampling bias and temporal heterogeneity in VAF measurements. For patients with very low baseline levels, small fluctuations in ctDNA levels over time could lead to large, calculated percent changes, potentially affecting the accuracy of response prediction. Few studies utilized in-depth comprehensive genomic profiling and calculated mean VAF from all detected variants (Supplementary Fig. 7*A* and *B*). Moreover, computing equally weighted sums of ctDNA VAF ratio change can skew results[11,12]; for example, a decrease from 50% to 5% VAF is treated similarly to a decrease from 1% to 0.1%, despite the latter being more susceptible to fluctuations. To overcome these limitations, we developed a novel model that accounts for VAF variance and sequencing depth, improving MinerVa-Delta's accuracy across different platforms. At a 30% threshold, MinerVa-Delta outperformed mean VAF-based metrics in predicting OS in two independent cohorts.

Another major clinical challenge is determining whether a patient with a radiologic stable disease is truly benefiting from treatment. Radiologic stable disease includes individuals with slowly progressive disease, indolent nonresponding disease, and radiologically subtle responses to treatment.[24] MinerVa-Delta may help distinguish between patients with indolent or progressing diseases who are unlikely to benefit from initial therapy, Therefore, it serves as a valuable complement to RECIST, aligning with findings from other studies.[11,13,33] Notably, MinerVa-Delta exhibited higher predictive accuracy in patients receiving PD-1 blockade plus chemotherapy compared with those receiving chemotherapy alone, suggesting it may be particularly useful in immunotherapy settings. In certain circumstances, tumor volume may not considerably decrease, and some patients may even experience tumor enlargement, known as "pseudoprogression," but eventually benefit from PD-1 blockade treatment.[34] In our model, patients with radiologic stable disease achieving molecular response are the "true" beneficiaries, whereas those classified as molecular nonresponders could be considered for escalated treatment. This dual functionality could also be valuable in early-phase clinical trials by providing an additional assessment of clinical benefit.

This proof-of-concept study highlights a noteworthy feature of MinerVa-Delta: its effectiveness through two strategies. Specifically, MinerVa-Delta tracks posttreatment variants using previous knowledge derived from either plasma or tumor tissue. By implementing these two strategies, we found the comparable performance of MinerVa-Delta in differentiating patients into molecular response and nonresponse groups. Furthermore, our observation indicates that the tumor tissue-informed strategy enhances pretreatment ctDNA detection rates compared with the plasma-informed method. Consequently, if biopsies are available, the tumor tissue-informed strategy should be preferred. Meanwhile, a tumor-agnostic strategy proposed by Zhang et al.[11] used a VAF threshold of 0.3% to minimize the background noise. However, this approach resulted in retaining only

Univariate forest plots comparing the prognostic performance of MinerVa-Delta and RECIST evaluation across all patients and treatment arms for PFS (*A*) and OS prediction (*B*). The number of responders, HR, 95% CI and *p* values are indicated. PFS, progression-free survival; CI, confidence interval; OS, overall survival; HR, hazard ratio; CI, confidence interval; RECIST, Response Evaluation Criteria in Solid Tumors; PD-1, programmed death-ligand 1.

a limited number of variants. Exceptions were made for variants with VAF less than 0.3% if detected in both pretreatment and posttreatment samples. Conversely, our study observed posttreatment plasma variations with VAFs as low as 0.01% after filtering CH variants, thereby improving assay sensitivity.

Several limitations of this study should be taken into account, including its retrospective nature. Although results were derived from two independent cohorts and the sample size was large (n = 227 and n = 97), these findings need validation in external cohorts or prospective studies. In addition, as chemotherapy alone is no longer the standard of care for patients with advanced LUSC, the relevance of cohort B's data in the current treatment landscape is limited. Nevertheless, cohort B provided valuable insights for validating the MinerVa-Delta model. Finally, the enrolled patients only included those with advanced LUSC, the predictive and prognostic role MinerVa-Delta warrants future investigations in patients with adenocarcinoma receiving first-line PD-1 blockade plus chemotherapy or targeted therapy.

In summary, MinerVa-Delta, which quantitatively assesses ctDNA dynamic changes, complements image-based RECIST by providing additional molecular information that enhances treatment response evaluation and guides personalized cancer care. Integrating ctDNA profiles with traditional imaging can lead to a more comprehensive and accurate assessment of treatment responses and disease status, particularly for patients with radiologic stable disease receiving PD-1 blockade plus chemotherapy.

CRediT Authorship Contribution Statement

Zhou Fei: Conceptualization, Writing - review & editing.

Huang S.Yu: Conceptualization, Methodology.

Chen Weizhi: Conceptualization, Writing - review & editing.

Zhou Caicun: Project administration, Resources.

Zhang Jiao: Data curation; Formal analysis.

Xu Li-Di: Supervision, Roles/Writing - original draft.

Li Feifei: Validation; Visualization.

Ma Ting: Validation; Visualization.

All the listed authors affiliated with institutes: Resources; data curation, and clinical data management in the Camel-Seq and LIPUSU studies. All the authors read and approved the final manuscript.

Data Availability Statement

The data sets used and/or analyzed during the current study are available from the corresponding author on reasonable request.

Disclosure

Dr. C. Zhou has received honoraria as a speaker for Lily China, Sanofi, Boehringer Ingelheim, Roche, MSD, Qilu, Hengrui, Innovent Biologics, C-Stone, LUYE Pharma, TopAlliance Biosciences Inc., Amoy Diagnositics, and is an advisor for Innovent Biologics, Hengrui, Qilu, and TopAlliance Biosciences Inc. Mrs. J. Zhang, Mrs. F. Li, Mrs. T. Ma, Dr. YS. Huang, Dr. L.-D. Xu, and Dr. W. Chen are employees of Genecast Biotechnology Co., Ltd. The remaining authors declare no conflict of interest.

Acknowledgments

The authors thank patients and their families for their participation and contributions to the CameL-Sq and LIPUSU clinical trials. This study is supported in part by the Natural Science Foundation of Shanghai (23ZR1453500), the New Quality Clinical Specialty Program of High-end Medical Disciplinary Construction in Shanghai Pudong New Area (2025-PWXZ-02), and the Healthcare Talents Youth Program of Shanghai Pudong New Area (2025PDWSYCQN-08).

Supplementary Data

Note: To access the supplementary material accompanying this article, visit the online version of the *Journal of Thoracic Oncology* at www.jto.org and at https://doi.org/10.1016/j.jtho.2025.05.021

References

1. Inoue A, Ota S, Yamasaki M, Batsaikhan B, Furukawa A, Watanabe Y. Gastrointestinal stromal tumors: a comprehensive radiological review. *Jpn J Radiol*. 2022;40:1105–1120.
2. Kaira K, Yamaguchi O, Naruse I, et al. Comparative analysis of different response criteria at early phase after PD-1 blockade in non-small lung cancer. *Cancer Imaging*. 2023;23:23.
3. Somarouthu B, Lee SI, Urban T, Sadow CA, Harris GJ, Kambadakone A. Immune-related tumour response assessment criteria: a comprehensive review. *Br J Radiol*. 2018;91:20170457.
4. Chiou VL, Burotto M. Pseudoprogression and immune-related response in solid tumors. *J Clin Oncol*. 2015;33:3541–3543.
5. Katz SI, Hammer M, Bagley SJ, et al. Radiologic pseudoprogression during anti-PD-1 therapy for advanced non-small cell lung cancer. *J Thorac Oncol*. 2018;13:978–986.
6. Hodi FS, Hwu WJ, Kefford R, et al. Evaluation of immune-related response criteria and RECIST v1.1 in patients with advanced melanoma treated with pembrolizumab. *J Clin Oncol*. 2016;34:1510–1517.
7. Moding EJ, Liu Y, Nabet BY, et al. Circulating tumor DNA dynamics predict benefit from consolidation immunotherapy in locally advanced non-small cell lung cancer. *Nat Cancer*. 2020;1:176–183.

ARTICLE IN PRESS

8. Thompson JC, Scholes DG, Carpenter EL, Aggarwal C. Molecular response assessment using circulating tumor DNA (ctDNA) in advanced solid tumors. *Br J Cancer*. 2023;129:1893–1902.
9. Riediger AL, Dietz S, Schirmer U, et al. Mutation analysis of circulating plasma DNA to determine response to EGFR tyrosine kinase inhibitor therapy of lung adenocarcinoma patients. *Sci Rep*. 2016;6:33505.
10. Parikh AR, Mojtahed A, Schneider JL, et al. Serial ctDNA monitoring to predict response to systemic therapy in metastatic gastrointestinal cancers. *Clin Cancer Res*. 2020;26:1877–1885.
11. Zhang Q, Luo J, Wu S, et al. Prognostic and predictive impact of circulating tumor DNA in patients with advanced cancers treated with immune checkpoint blockade. *Cancer Discov*. 2020;10:1842–1853.
12. Thompson JC, Carpenter EL, Silva BA, et al. Serial monitoring of circulating tumor DNA by next-generation gene sequencing as a biomarker of response and survival in patients with advanced NSCLC receiving pembrolizumab-based therapy. *JCO Precis Oncol*. 2021;5:PO.20.00321.
13. Tie J, Kinde I, Wang Y, et al. Circulating tumor DNA as an early marker of therapeutic response in patients with metastatic colorectal cancer. *Ann Oncol*. 2015;26:1715–1722.
14. Goldberg SB, Narayan A, Kole AJ, et al. Early assessment of lung cancer immunotherapy response via circulating tumor DNA. *Clin Cancer Res*. 2018;24:1872–1880.
15. Osumi H, Shinozaki E, Yamaguchi K, Zembutsu H. Early change in circulating tumor DNA as a potential predictor of response to chemotherapy in patients with metastatic colorectal cancer. *Sci Rep*. 2019;9:17358.
16. Vega DM, Nishimura KK, Zariffa N, et al. Changes in circulating tumor DNA reflect clinical benefit across multiple studies of patients with non-small-cell lung cancer treated with immune checkpoint inhibitors. *JCO Precis Oncol*. 2022;6:e2100372.
17. Bratman SV, Yang SYC, Iafolla MAJ, et al. Personalized circulating tumor DNA analysis as a predictive biomarker in solid tumor patients treated with pembrolizumab. *Nat Cancer*. 2020;1:873–881.
18. Nabet BY, Esfahani MS, Moding EJ, et al. Noninvasive early identification of therapeutic benefit from immune checkpoint inhibition. *Cell*. 2020;183:363–376.e13.
19. Xia L, Mei J, Kang R, et al. Perioperative ctDNA-based molecular residual disease detection for non-small cell lung cancer: a prospective multicenter cohort study (LUNGCA-1). *Clin Cancer Res*. 2022;28:3308–3317.
20. Sanz-Garcia E, Zhao E, Bratman SV, Siu LL. Monitoring and adapting cancer treatment using circulating tumor DNA kinetics: current research, opportunities, and challenges. *Sci Adv*. 2022;8:eabi8618.
21. Ren S, Chen J, Xu X, et al. Camrelizumab plus carboplatin and paclitaxel as first-line treatment for advanced squamous NSCLC (CameL-Sq): a phase 3 trial. *J Thorac Oncol*. 2022;17:544–557.
22. Xia L, Pu Q, Kang R, et al. Dynamic ctDNA to inform the precise management of resected NSCLC: LUNGCA-2 study. *J Clin Oncol*. 2023;41:8528.
23. Jakobsen AKM, Spindler KG. ctDNA-response evaluation criteria in solid tumors - a new measure in medical oncology. *Eur J Cancer*. 2023;180:180–183.
24. Eisenhauer EA, Therasse P, Bogaerts J, et al. New response evaluation criteria in solid tumours: revised RECIST guideline (version 1.1). *Eur J Cancer*. 2009;45:228–247.
25. Deveson IW, Gong B, Lai K, et al. Evaluating the analytical validity of circulating tumor DNA sequencing assays for precision oncology. *Nat Biotechnol*. 2021;39:1115–1128.
26. Zhang J, Pan Y, Shi Q, et al. Paclitaxel liposome for injection (Lipusu) plus cisplatin versus gemcitabine plus cisplatin in the first-line treatment of locally advanced or metastatic lung squamous cell carcinoma: a multicenter, randomized, open-label, parallel controlled clinical study. *Cancer Commun (Lond)*. 2022;42:3–16.
27. Kamarudin AN, Cox T, Kolamunnage-Dona R. Time-dependent ROC curve analysis in medical research: current methods and applications. *BMC Med Res Methodol*. 2017;17:53.
28. Parkinson CA, Gale D, Piskorz AM, et al. Exploratory analysis of TP53 mutations in circulating tumour DNA as biomarkers of treatment response for patients with relapsed high-grade serous ovarian carcinoma: a retrospective study. *PLoS Med*. 2016;13:e1002198.
29. Abbosh C, Frankell AM, Harrison T, et al. Tracking early lung cancer metastatic dissemination in TRACERx using ctDNA. *Nature*. 2023;616:553–562.
30. Jiang T, Jiang L, Dong X, et al. Utilization of circulating cell-free DNA profiling to guide first-line chemotherapy in advanced lung squamous cell carcinoma. *Theranostics*. 2021;11:257–267.
31. O'Leary B, Hrebien S, Morden JP, et al. Early circulating tumor DNA dynamics and clonal selection with palbociclib and fulvestrant for breast cancer. *Nat Commun*. 2018;9:896.
32. Hrebien S, Citi V, Garcia-Murillas I, et al. Early ctDNA dynamics as a surrogate for progression-free survival in advanced breast cancer in the BEECH trial. *Ann Oncol*. 2019;30:945–952.
33. Assaf ZJF, Zou W, Fine AD, et al. A longitudinal circulating tumor DNA-based model associated with survival in metastatic non-small-cell lung cancer. *Nat Med*. 2023;29:859–868.
34. Lee JH, Long GV, Menzies AM, et al. Association between circulating tumor DNA and pseudoprogression in patients with metastatic melanoma treated with anti-programmed cell death 1 antibodies. *JAMA Oncol*. 2018;4:717–721.